Received: 12 May 2024 | Revised: 27 November 2024 | Accepted: 31 March 2025 | Published online: 18 April 2025

RESEARCH ARTICLE

Journal of Optics and Photonics Research
2025, Vol. 00(00) 1–8
DOI: 10.47852/bonviewJOPR52023409

BON VIEW PUBLISHING

Band Gap Modulation and Optical Property Enhancement in Sn-Doped CuO Nanostructures for Advanced Optoelectronic Applications

Muhammad Idrees[1], Salman Khan[2] and Saddam Hussain[1,*]

[1]*School of Physics, Beijing Institute of Technology, China*

[2]*School of Chemical Engineering, Beijing Institute of Technology, China*

Abstract: Optical properties play a crucial role in diverse applications. However, the optical characteristics of materials are determined by their structure and composition. This study focused on nanostructured materials, which exhibit enhanced optical properties compared to their bulk counterparts. Specifically, copper oxide (CuO) and Sn-doped CuO materials were experimentally synthesized using the hydrothermal method. The CuO and Sn-doped CuO nanostructure materials were subsequently compared, and their optical characteristics and structural composition were investigated using various analytical techniques, including photoluminescence spectroscopy (PL), scanning electron microscopy (SEM), and ultraviolet-visible spectroscopy (UV-Vis). A significant finding of this study is that doping can be utilized to modulate the band gap of materials and enhance their optical characteristics. The investigation revealed that CuO has a band gap of 2.5 eV. However, doping decreased the band gap; the band gap of synthesized CuO is 3.1 eV, which decreases with the doping of Sn to 2.1 eV, consequently improving the material's optical characteristics. This experimental investigation in optics demonstrates the enhancement of a material's optical qualities through band gap reduction via doping. Furthermore, potential real-world applications for these materials in fabricating LEDs and photodetectors were discussed. With their improved optical characteristics, these materials could be utilized in various optical applications such as sensors, displays, and solar cells. In conclusion, this study contributes to the existing knowledge regarding enhancing optical properties in nanostructured materials and their potential applications in real-world contexts.

Keywords: enhancement of optical properties, copper oxide, Tin-doped copper oxide

1. Introduction

Nanostructured materials offer a multiplicity of applications in the optical field because their band gap is smaller than that of bulk materials. The small band gap in copper oxide (CuO), which can be synthesized in different sizes, shapes, and morphologies in the visible light region, opens new prospects for developing optical technologies. Hundreds of scientists focus on developing nanomaterials for several uses, especially in industrially developed contemporary engineering applications. This emphasis is mainly due to the considerable improvements in nanotechnology and nanostructure developments during the last decade. These materials are applied in optical electronic devices, photocatalysis, and the conversion of solar energy, photoconductive materials, and photothermal uses. The addition of tin into CuO improves the optical properties to enable suitable size, shape, and band gap modifications for application into different optical devices [1, 2].

Regarding semiconductors, CuO belongs to a p-type semiconductor composed of a small band gap ranging from 1.8 eV to 2.5 eV [3–6]. This material is utilized actively in numerous applications, such as thermal conductivity, glucose sensor circuitries, and lithium-ion batteries. Besides, it can be employed in a magnetic storage medium. Several strategies synthesize CuO, including sol-gel, chemical pretreatment, simple pretreatment, and aqueous solution methods. Scientists today are interested in nanoscale transition metal oxides. This surge in attention can be attributed to the expansive diversity of nanomaterials compared to bulk materials. Their properties encompass nearly all facets of science and physics in materials, showcasing remarkable chemical and physical characteristics. CuO, recognized as a prominent p-type semiconductor, has become increasingly appealing due to its wide array of potential applications. Several studies have explored enhancing optical and structural properties through doping and synthesis techniques. For instance, El Sayed et al. [7] investigated the effects of co-doping CuO with Sn and Zn, demonstrating improved magneto-optical and corrosion-resistant properties. However, their focus was primarily on co-doping and corrosion inhibition, with less emphasis on optical enhancements for optoelectronics. Our work diverges by targeting single-element Sn doping to reduce the band gap and enhance optical absorption properties for optoelectronic applications. Furthermore, our study incorporates computational simulations to optimize light absorption, an aspect not addressed in their work.

Similarly, while Mohebbi et al. [8] studied Sn-doped CuO nanoparticles synthesized via a hydrothermal method, they analyzed structural and optical properties (e.g., XRD, photoluminescence (PL), FT-IR). Unlike Mohebbi et al., which focused on basic optical

*Corresponding author: Saddam Hussain, School of Physics, Beijing Institute of Technology, China. Email: 3820202051@bit.edu.cn

enhancements, they observed a blue shift in PL spectra and reported particle size increases from 16 nm (pure CuO) to 22 nm (Sn-doped CuO).

Our study investigates similar enhancements and achieves smaller nanoparticle sizes (19 nm for CuO and 30 nm for Sn-doped CuO), improving light absorption for specific optoelectronic applications. He also reported structural stability after Sn doping but did not extend their findings to practical device fabrication. We connect the optical enhancements to applications like solar cells and photodetector, validated by computational simulations. It is worth noting that Jan et al. [9] SnxCu1-xO (where x = 0,0.04, 0.06 & 0.10) nanostructures have been prepared via co-precipitation technique and characterized for different physiochemical properties and anticancer activity. In our work, we use the hydrothermal method to enhance the optical properties of CuO through Sn doping for optoelectronic applications. Doping is crucial for modifying material properties, enhancing surface qualities, reducing particle size, and altering shapes [10, 11]. This process can significantly improve various attributes of CuO, including its electrical, optical, magnetic, and bioactive properties. Moreover, doping influences the morphological features of CuO by facilitating an exchange between the s and p electrons of the host CuO and the d electrons of the doped material [12, 13]. Additionally, the optical and antibacterial properties of CuO nanostructures are significantly improved through doping treatments [14].

Previous research examined nanoparticle sizes ranging from 93 to 44 nm for the Cu1-2xSnxZnxO structure. The CuO nanoparticles detected in this study were 19 nm, while Sn-doped CuO was 30 nm. Compared to the Cu1-2xSnxZnxO, they are much smaller (19–30 nm) than the nanostructures produced in this investigation. Consequently, this work mainly focused on the impact of Sn doping on optical characteristics and prospect use in optoelectronics. The new features of this work are the attempts to minimize the band gap and improve the optical properties together with the simulation of light absorption to make an addition to the experimental part and introduce computational aspects to the work.

In this respect, Sn doping is preferred over the other dopants because it improves the PL properties, band gap engineering, compatibility, solubility, and chemical stability. The hydrothermal method is favored for its precise control of morphology and size, high purity/crystallinity, low-temperature synthesis, homogenous doping, using environmentally friendly materials and scalability. Therefore, we have focused on examining the various properties of these nanostructures and evaluating the results against undoped CuO nanostructures synthesized via the same route.

2. Materials and Methodology

This part will describe the hydrothermal method used to produce CuO and Sn-doped CuO (Sn). Several characterization techniques will be employed to analyze the samples.

2.1. Fabrication of CuO and Sn-doped CuO

CuO and Sn-doped CuO were synthesized by using various techniques [15]. We are currently employing the hydrothermal approach in our operations.

2.1.1. Materials

The materials for synthesizing CuO and Sn-doped CuO are $CuCl_2$, NaOH, KOH, $SnCl_2$, deionized water, and distilled water as solvents.

2.1.2. Methodology

The hydrothermal technique is used to manufacture CuO and Sn-doped CuO [16]. This relatively simple procedure illustrates the various concentrations found in the two samples in Tables 1 and 2.

2.1.3. Preparation of sample 1

To complete the operation, you must agitate two distinct solutions, NaOH and KOH, for thirty minutes each. The two solutions are combined into the $CuCl_2$ solution drop by drop and then agitated for sixty minutes until they become a homogeneous and consistent mixture. This process is repeated until the two solutions are ready. A blue hue will be produced by the solution that is created. Following this step, the blue solution is transported into an autoclave lined with Teflon and then placed in an oven at a temperature of 180 degrees Celsius for twenty hours. Following the completion of the reaction, the water and particles are separated through centrifugation. After that, the particles are washed with ethanol and distilled water to eliminate any more particles that may have been left behind. In conclusion, filter paper is utilized for filtration to separate any particles that may still be present thoroughly. After filtration, the particles are dried at a temperature of sixty degrees Celsius for sixty minutes [16].

2.1.4. Preparation of sample 2

Doping CuO with tin is a straightforward process that utilizes the hydrothermal method [17]. The first three solutions produced are presented in Table 2.

It is recommended that each solution be stirred for thirty minutes. The first two solutions should be combined and swirled for thirty minutes. The third solution should be added gradually, drop by drop, while stirring continually until the solution is consistent. It is recommended that the final solution be a grayish color. After the solution has been made, it is placed in an autoclave lined with Teflon. The autoclave is then placed in an oven for eighteen hours. When the reaction is finished, the particles and water are separated using centrifugation to separate them, respectively. After being filtered, the particles are washed with deionized water and ethanol to remove surplus particles. After this step, the particles are dried at a

Table 1
Shows a detailed description of synthesized CuO

1^{st} solution	$CuCl_2 = 0.1$ M	Distilled water = 25 ml	$CuCl_2 = 0.16$ g
2^{nd} solution	NaOH = 0.3 M	Distilled water = 12.5 ml	NaOH = 0.1 g
3^{rd} solution	KOH = 0.3 M	Distilled water = 12.5 ml	KOH = 0.1 g

Table 2
Shows a detailed description of synthesized Sn-doped CuO

1^{st} solution	$CuCl_2 = 0.1$ M	Deionized water = 25 ml	$CuCl_2 = 0.16$ g
2^{nd} solution	KOH = 0.3 M	Deionized water = 15 ml	KOH = 0.1 g
3^{rd} solution	$SnCl_2 = 0.1$ M	Deionized water = 10 ml	$SnCl_2 = 0.08$ g

temperature of sixty degrees Celsius for sixty minutes. A digital balance is one of the pieces of equipment utilized to determine the quantity of salts. A magnetic hot plate is utilized to produce a homogeneous solution. An autoclave of steel vessels lined with Teflon is used to grow nanoparticles. The separation of nanoparticles and water is accomplished with the help of a centrifuge machine. Filter paper is utilized to filter the excess particles from the manufactured product. In addition to being used for the reaction, the oven is used to heat and dry the fragments.

3. Result and Discussion

3.1. Scanning electron microscope

The synthesized CuO and Sn-doped CuO were analyzed using scanning electron microscopy (SEM) for research purposes. SEM allows for examining the surface structure, shape, and size of the produced nanostructures by detecting electrons emitted from the molecules. Various images were captured at different resolutions, revealing that the nanostructures had an average diameter of approximately 100 nanometers. Using ImageJ software, the size of the CuO nanostructures was observed to be smaller than that of the Sn-doped CuO nanostructures. Specifically, the diameter of the CuO nanostructures was around 19 nm, as illustrated in Figure 1(a–e). In contrast, the doping of Sn resulted in an increase in the average size of the Sn-doped CuO nanostructures to 30 nm. This finding was consistent with the X-ray diffraction (XRD) data.

3.2. XRD

XRD is a technique used to determine prepared samples' size, spacing, and shape. By analyzing the diffraction patterns from various angles, we can obtain Miller indices, which are instrumental in identifying the monoclinic phases of CuO. To calculate particle size, we apply the Scherrer formula. This formula can be expressed as:

$$D = k\lambda/\beta cos\theta \tag{1}$$

The letter k represents the constant 0.9, λ denotes the X-ray wavelength (1.5418 Å), and θ refers to the Bragg diffraction angle. The letter k represents the continuous 0.9, λ denotes the X-ray wavelength (1.5418 Å), and θ refers to the Bragg diffraction angle [18].

From the XRD analysis in Table 3 from Figure 2(a), we calculated the average size of CuO using the Scherrer formula, which is 19 nm.

According to the XRD study of Sn-doped CuO nanostructures, the structure of the CuO material is not altered by the presence of Sn doping. Sn doping, on the other hand, reduces the amount of noise while increasing the nanostructures' size. Based on the results of the XRD investigation of Sn-doped CuO, the average size was determined to be 30 nanometers. Additional information can be found in Table 4.

3.3. Ultraviolet-visible spectroscopy (UV-Vis)

UV-Vis spectroscopy is a technique used to determine the absorbance of UV and visible light, facilitating research into the optical properties of synthesized nanostructures. Atoms and molecules can absorb light within the ultraviolet (UV) and visible spectrum when the energy of the radiation matches the energy difference between two electronic levels [19].

A UV-Vis spectrometer can confirm the presence of nanostructures by analyzing the optical absorption spectra associated with them. For example, the presence of CuO can be identified by an absorption peak between 240 and 330 nm in Figure 3(a) and (b). Each nanostructure has a broad absorption range from the UV to the visible spectrum. Additionally, doping

Figure 1
(a), (b) show SEM images with different resolutions of sample 1. (CuO with NaOH = 0.3 moles, $CuCl_2$ = 0.1 moles, and KOH = 0.3 moles). (c), (d) (e) shows SEM images with different resolutions (Sn-doped CuO is prepared with $Cucl_2$ = 0.1 moles, KOH = 0.3 moles, and $SnCl_2$ = 0.1 moles)

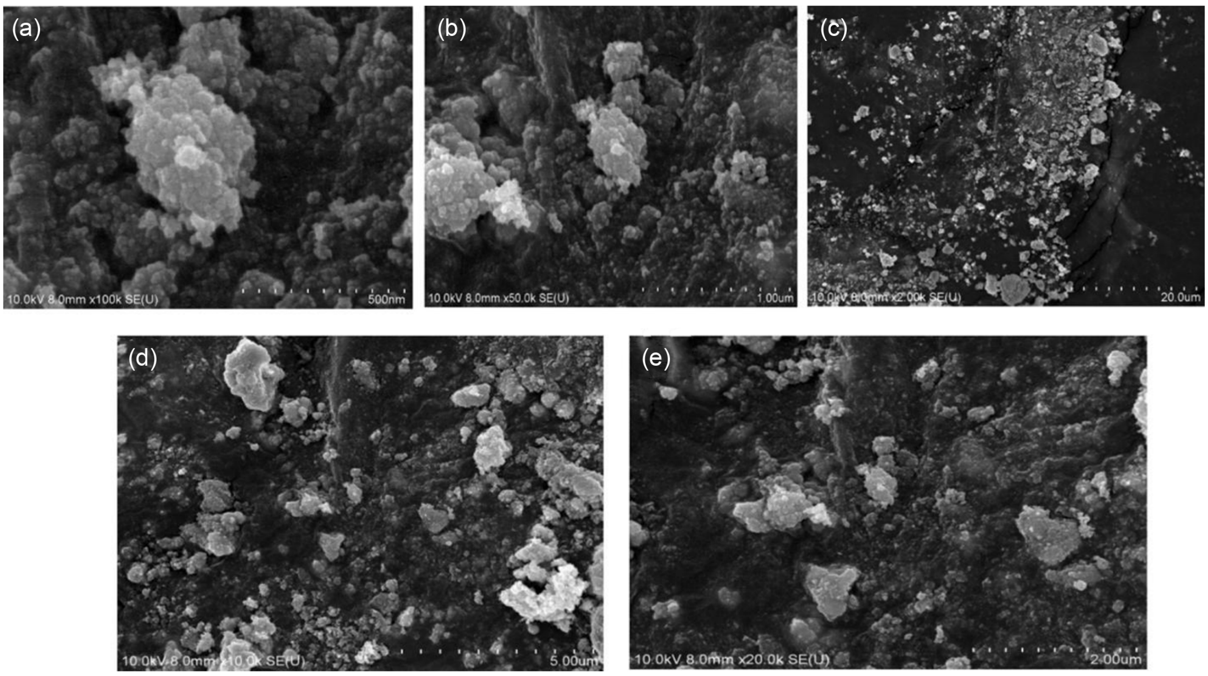

Table 3
Analysis of crystallographic peaks and particle size determination of CuO nanostructures

Peak (2Θ)	(hkl)	FWHM degree	FWHM radian	Particle size
20	101	0.41831	0.03721	19.19
28	011	0.29856	0.00723	23.76
32	110	0.38762	0.08712	27.91
38	111	0.56742	0.10981	15.23
53	200	0.56723	0.13421	13.21
57	202	0.87654	0.23901	21.11
60	210	0.84972	0.21765	25.10
64	311	0.98765	0.78265	13.30
67	113	0.2783	0.07865	12.09

Table 4
Crystallographic analysis and particle size estimation of Sn-doped CuO nanostructures

Peak (2Θ)	(hkl)	FWHM degree	FWHM radian	Particle size
28	101	0.07292	1.2726	32.98
36	011	0.25604	0.2365	28.23
40	111	0.79768	1.2748	32.10
42	200	0.20234	0.0341	26.87
44	201	0.8713	0.0072	22.24
50	200	0.81717	1.9821	37.91

Sn into CuO can extend the absorption peak range; Sn-doped CuO exhibits an absorption peak between 330 and 380 nanometers.

3.4. Energy-dispersive X-ray spectroscopy

Energy-dispersive X-ray analysis is a technique for determining a sample's elemental composition. This method employs X-rays generated by electron beams to extract detailed information about the chemicals.

As demonstrated by Shirley and Jarochowska, as well as Scimeca et al. [20, 21], in Figure 4, the EDX examination of the synthesized nanostructures confirms the presence of CuO, supported by visible peaks in the graph corresponding to the elements copper and oxygen. The carbon peak evident in the figure arises from using a carbon substrate on which the sample is positioned. Additionally, there is clear evidence that tin (Sn) has been successfully absorbed into the CuO, as demonstrated by the elemental peaks for copper, tin, and oxygen as shown in Figure 2(a) and (b). This indicates that the incorporation of tin into CuO has achieved its intended outcome. The sulfur signal is associated with impurities found in the salt, while the small carbon signal observed can be attributed to the equipment used for the sample presentation.

3.5. Photoluminescence spectroscopy

These figures illustrate that Sn doping employs the scientific technique known as PL spectroscopy. PL is used to analyze the optical characteristics of samples, primarily aimed at identifying defects, such as vacancies and impurities, that exist within the visible spectrum of materials [22, 23]. For instance, in the case of pure CuO nanostructures (Figure 5(a)), oxygen or copper impurities generate additional energy levels within the band gap, resulting in light emission from the sample. CuO is classified as a p-type semiconductor characterized by vacancies in the copper atoms, which facilitate this emission. Both copper and oxygen vacancies contribute to the light emitted in CuO, with the formation energy of these vacancies being similar to that of oxygen vacancies. The sharp PL emission peak observed between 280 nm and 350 nm reflects the radiative recombination of charge carriers, indicating the intrinsic optical behavior of pure CuO.

Figure 5(b), representing Sn-doped CuO nanostructures, demonstrates how the doping process slightly alters the intensity of the emitted light. The emission bands, extending from 270 nm to

Figure 2
(a) X-ray diffraction of pure copper oxide nanostructure and (b) X-ray diffraction of Sn-doped copper oxide

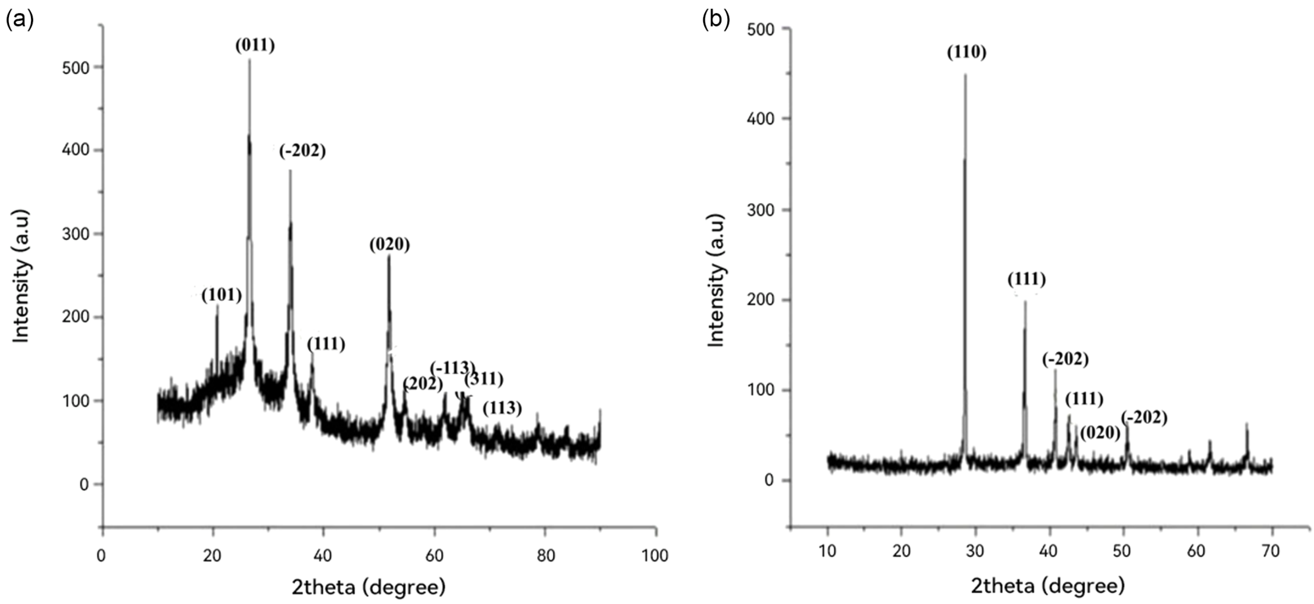

Figure 3
(a) UV-visible spectroscopy of pure copper oxide nanostructure and (b) UV-visible of Sn-doped copper oxide nanostructure

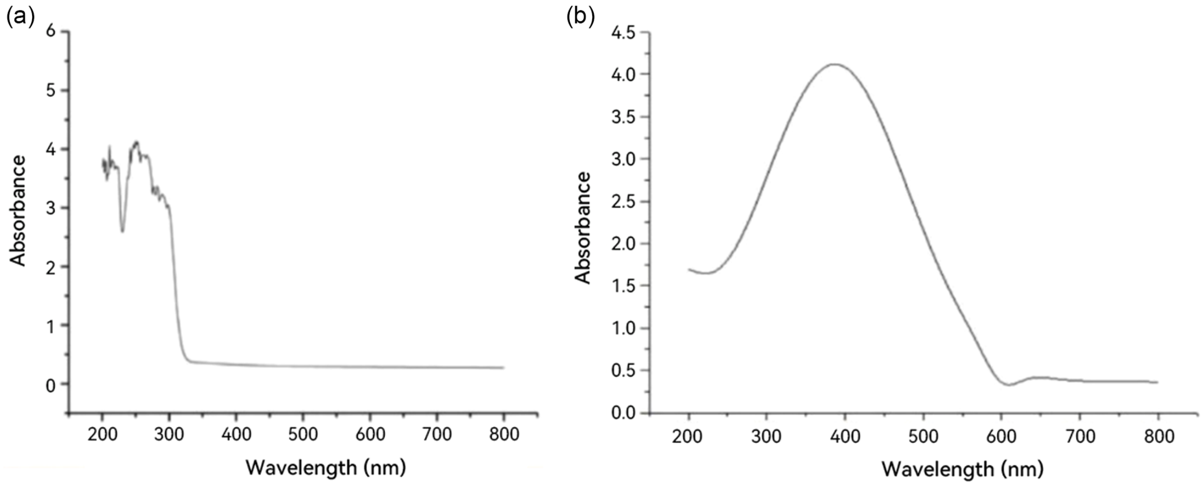

Figure 4
(a) EDX analysis of pure copper oxide nanostructure. (b) EDX analysis of Sn-doped Copper oxide nanostructure

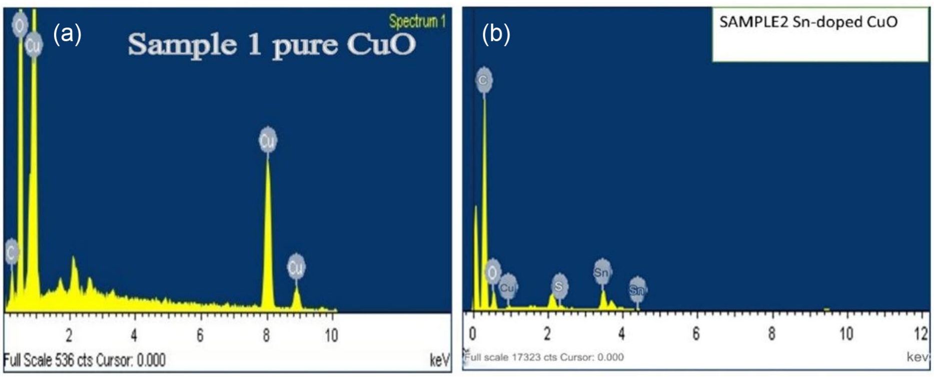

Figure 5
(a) Shows the PL of pure CuO nanostructure and (b) shows the PL of Sn-doped CuO nanostructure

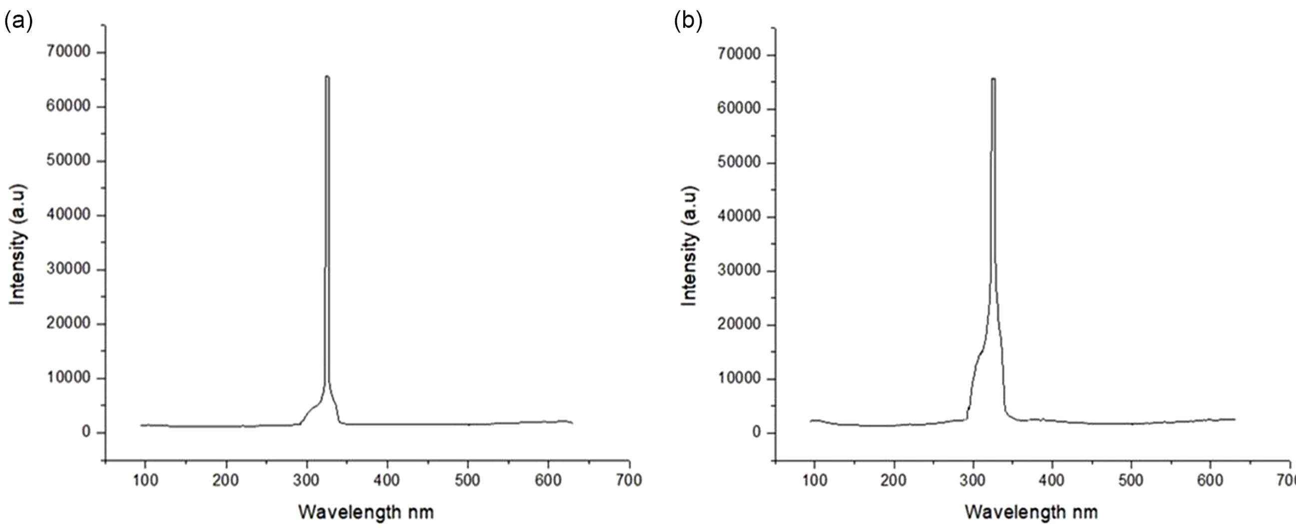

360 nm, highlight the effect of Sn incorporation on the electronic structure of CuO. The doping does not introduce new energy levels into the band structure of CuO but modifies the defect density and band gap characteristics. This results in subtle changes in the optical emission, attributed to the influence of Sn on the charge carrier dynamics and defect states.

In conclusion, while Sn doping leads to a minor modification in the intensity and emission range, it remains effective in slightly tuning the optical characteristics without fundamentally altering the band structure of CuO.

3.6. Application in optoelectronic device fabrication

The creation of light-emitting diodes and photodetectors with superior optical properties can be accomplished by synthesizing nanostructures of CuO and Sn-doped CuO [24, 25]. The design process for the simulation is carried out with the help of MATLAB, as depicted in Figure 6. This simulation analyzes the light absorption in the active zone of light-emitting diodes (Figure 6(a)) and the absorption layers of photodetectors (Figure 6(b)), providing information about the light absorption. It is essential to have this information to maximize the gadget's performance. There is a very high absorption (almost complete absorption, reaching the upper limit of the scale on the graph) in the UV range, specifically from about 200 nm to just under 300 nm. This indicates that the material in the LED's active region (Figure 6(a)) is highly efficient at absorbing UV light. Absorption sharply decreases following this range, reaching almost nothing, and stays low through the visible spectrum and into the near-infrared. The material used in the LED's active region appears to be specially designed to absorb UV light while allowing other wavelengths to flow through or reflect based on the measured absorption spectrum. This can signify a material composition ideal for UV emission-dependent applications, such as sterilization, medicinal procedures, or specific chemical reactions. Strong UV absorption combined with visible light transparency points to applications where regulated light outputs are required, maybe in multi-wavelength LED systems where various layers absorb and emit different portions of the spectrum. The outcome highlights the significance of material science in developing cutting-edge LED technologies by pointing to unique material features designed for specific optical applications. This absorption property is essential for enhancing the efficiency of LED-based gadgets and their range of applications.

The y-axis represents the absorption level (in arbitrary units) on a $\times 10^{-16}$ scale. The graph demonstrates that absorption remains constant at approximately 1.2×10^{-16} between 200 and 300 nm. Subsequently, it exhibits a sharp decline toward nearly zero, commencing at approximately 320 nm, maintaining this constant value afterward. This graphical representation illustrates that the LED's active region exhibits significant absorption in the UV range (approximately 300 nm) but minimal absorption in the visible and near-infrared spectra.

The x-axis represents wavelength (in nm) from 200 nm to 800 nm. The y-axis similarly depicts the absorption level on a comparable scale to the first graph, with mean values approximating 2.5×10^{-16} (Figure 6(b)). In a range of 200 nm and 300 nm, the absorption starts at an elevated level of 2.5×10^{-16}, which subsequently descends sharply and levels off to around the value of 1×10^{-16} at a broad range up to 800 nm. This graph shows that the absorbing layer of the present photodetector has a high absorption coefficient in the UV region and a sound absorption coefficient in the visible and near-infrared regions. In contrast, the LED only has a high absorption coefficient in the UV region.

These characteristics indicate that the LED has been designed for effective emission in the visible or near UV region with a slight reabsorption loss. On the other hand, the photodetector has broader absorption, which ranges from the UV region and up to the visible and near-IR wavelength range, therefore suitable for multiple wavelength detection. Hence, the LED works within a specific range, experiencing little or no reabsorption losses, and the photodetector, apart from detecting a wide range of wavelengths, can operate independently of the LED. Through the absorption properties analysis, the photodetector's absorbing layer is optimized for UV and visible region up to the green area, and the cutoff wavelength is estimated to be around the blue-green boundary. This might be because the material's electrical

Figure 6
(a) LED active region absorption 1.5 m^{-1} and (b) photodetector active layers absorption 2.4 m^{-1}

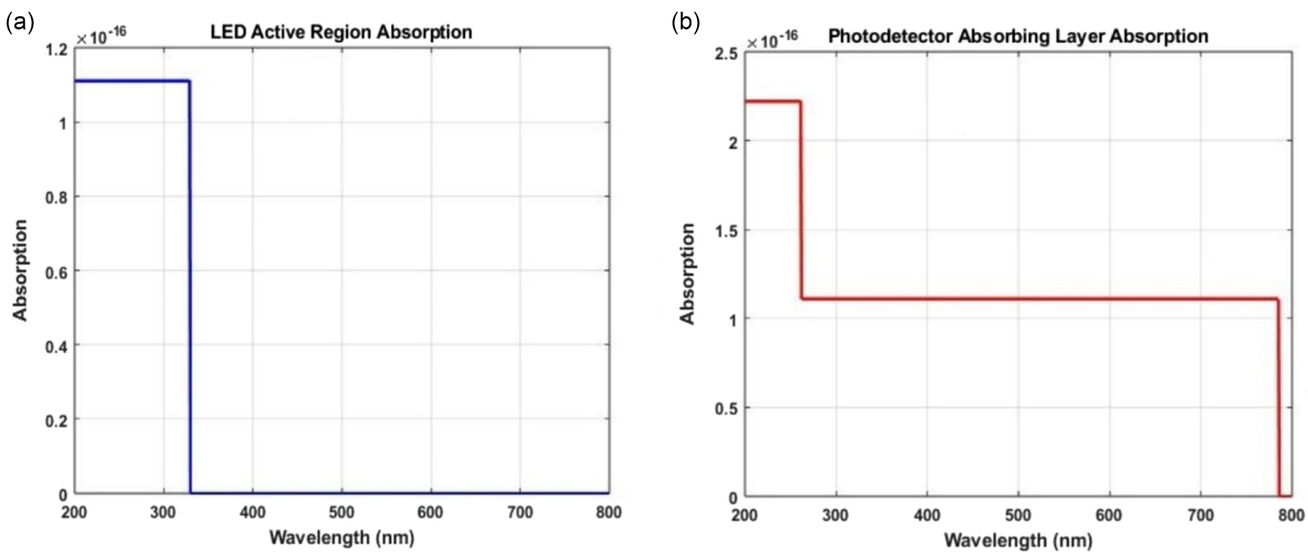

characteristic bars its ability to capture longer infrared wavelengths. This means the photodetector's performance is ideal for detecting visible and UV light, not red or infrared. This can be important, for example, if the dye exhibits fluorescence, which is essential for visible and UV light but unwanted for infrared light. Suppose more layers or even modifications of existing materials are required to bring the cutting edge of the photodetector further into longer wavelengths for a given application. In that case, more work may be done in this field. Refining the design of a photodetector to maximize its efficiency and response time for the target wavelengths requires a thorough understanding of the material's absorption properties. This absorption profile provides valuable information about the spectral sensitivity of the photodetector's absorbing layer, highlighting its capabilities and limitations, which are crucial for tailoring the device to specific applications.

4. Conclusion

Various solutions were employed to synthesize the nanostructures of CuO and Sn-doped CuO, after which the properties of these nanostructures from different solutions were compared. The research revealed that the size of CuO was 19 nanometers, whereas the size of Sn-doped CuO was 30 nanometers. Furthermore, the band gaps of both structures shifted from 3.1 electron volts to 2.1 electron volts. Additionally, it was observed that the optical properties of the material could be enhanced by decreasing the size of the band gap. As doping tin with CuO has resulted in novel applications in optics, this method is considered an innovative approach with potential applications in producing optoelectronic devices. The synthesized nanostructures of CuO and Sn-doped CuO have potential applications in the fabrication of light-emitting diodes with enhanced optical characteristics. Simulations were conducted using MATLAB to determine the light absorption in the active region of light-emitting diodes and the absorption layers of photodetectors. This information is essential for optimizing device performance.

Ethical Statement

This study contains no studies with human or animal subjects performed by any authors.

Conflicts of Interest

The authors declare that they have no conflicts of interest in this work.

Data Availability Statement

Data are available from the corresponding author upon reasonable request.

Author Contribution Statement

Muhammad Idrees: Conceptualization, Methodology, Validation, Formal analysis, Investigation, Resources, Data curation, Writing – original draft, Writing – review & editing. **Salman Khan:** Software, Validation, Investigation, Visualization, Supervision, Project administration. **Saddam Hussain:** Software, Validation, Investigation, Visualization, Supervision, Project administration.

References

[1] Diachenko, O., Kováč Jr, J., Dobrozhan, O., Novák, P., Kováč, J., Skriniarova, J., & Opanasyuk, A. (2021). Structural and optical properties of CuO thin films synthesized using spray pyrolysis method. *Coatings*, *11*(11), 1392. https://doi.org/10.3390/COATINGS11111392

[2] Maciulis, V., Ramanaviciene, A., & Plikusiene, I. (2022). Recent advances in synthesis and application of metal oxide nanostructures in chemical sensors and biosensors. *Nanomaterials*, *12*(24), 4413. https://doi.org/10.3390/NANO12244413

[3] Ajjaq, A., Barin, Ö., Çağırtekin, A. O., Soltabayev, B., & Acar, S. (2023). ZnO seed-mediated hydrothermal growth of advanced 1-D ZnO and 2-D CuO nanostructured oxide ceramics for gas sensing applications. *Ceramics International*, *49*(24), 40853–40865. https://doi.org/10.1016/J.CERAMINT.2023.10.071

[4] Zhang, X., Zhang, D., Ni, X., & Zheng, H. (2008). Optical and electrochemical properties of nanosized CuO via thermal decomposition of copper oxalate. *Solid-State Electronics*, *52*(2), 245–248. https://doi.org/10.1016/j.sse.2007.08.009

[5] Baran, T., Visibile, A., Busch, M., He, X., Wojtyla, S., Rondinini, S., . . . , & Vertova, A. (2021). Copper oxide-based photocatalysts and photocathodes: Fundamentals and recent advances. *Molecules*, *26*(23), 7271. https://doi.org/10.3390/MOLECULES26237271

[6] Moumen, A., Kumarage, G. C. W., & Comini, E. (2022). P-type metal oxide semiconductor thin films: Synthesis and chemical sensor applications. *Sensors*, *22*(4), 1359. https://doi.org/10.3390/s22041359

[7] El Sayed, M. Y., El Ghouch, N., Younes, G. O., & Awad, R. (2023). Structural, morphological, and magneto-optical investigations of pure and (Sn, Zn) co-doped CuO nanoparticles: A novel corrosion inhibitor in acidic media. *Materials Today Communications*, *35*, 105490. https://doi.org/10.1016/j.mtcomm.2023.105490

[8] Mohebbi, S., Molaei, S., & Judy, A. A. R. (2013). Preparation and study of Sn-doped CuO nanoparticles as semiconductors. *Journal of Applied Chemistry*, *8*(27), 27–30.

[9] Jan, T., Iqbal, J., Farooq, U., Gul, A., Abbasi, R., Ahmad, I., & Malik, M. (2015). Structural, Raman and optical characteristics of Sn doped CuO nanostructures: A novel anticancer agent. *Ceramics International*, *41*(10), 13074–13079. https://doi.org/10.1016/j.ceramint.2015.06.080

[10] Chen, J., Fang, S., Shen, Q., Fan, J., Li, Q., & Lv, K. (2022). Recent advances of doping and surface modifying carbon nitride with characterization techniques. *Catalysts*, *12*(9), 962. https://doi.org/10.3390/catal12090962

[11] Yoo, H., Heo, K., Ansari, M. H. R., & Cho, S. (2021). Recent advances in electrical doping of 2D semiconductor materials: Methods, analyses, and applications. *Nanomaterials*, *11*(4), 832. https://doi.org/10.3390/nano11040832

[12] Phuruangrat, A., Thongtem, T., & Thongtem, S. (2024). Combustion synthesis of Ce/Mg co-doped ZnO nanoparticles as a visible-light-driven photocatalyst. *Journal of Ovonic Research*, *20*(2), 177–185. https://doi.org/10.15251/JOR.2024.202.177

[13] Thangamani, C., Ponnar, M., Priyadharshini, P., Monisha, P., Gomathi, S. S., & Pushpanathan, K. (2019). Magnetic behavior of Ni-doped CuO nanoparticles synthesized by microwave irradiation method. *Surface Review and Letters*, *26*(5), 1850184. https://doi.org/10.1142/S0218625X18501846

[14] Singh, B. P., Chaudhary, M., Kumar, A., Singh, A. K., Gautam, Y. K., Rani, S., & Walia, R. (2020). Effect of Co and Mn doping on the morphological, optical and magnetic properties of CuO nanostructures. *Solid State Sciences*, *106*, 106296. https://doi.org/10.1016/J.SOLIDSTATESCIENCES.2020.106296

[15] Ben Nasr, F., Mnif, S., Guermazi, H., Duponchel, B., Leroy, G., Aifa, S., & Guermazi, S. (2024). Synthesis, characterization of (Fe, Sn)

doped and co-doped copper oxide nanoparticles and evaluation of their antibacterial activities. *Journal of Cluster Science*, *35*, 1827–1843. https://doi.org/10.1007/s10876-024-02613-0

[16] Hemalatha, T., Akilandeswari, S., Krishnakumar, T., Leonardi, S. G., Neri, G., & Donato, N. (2019). Comparison of electrical and sensing properties of pure, Sn-and Zn-doped CuO gas sensors. *IEEE Transactions on Instrumentation and Measurement*, *68*(3), 903–912. https://doi.org/10.1109/TIM.2018.2852538

[17] Peddi, P., Ptsrk, P. R., Rani, N. U., & Tulasi, S. L. (2021). Green synthesis, characterization, antioxidant, antibacterial, and photocatalytic activity of *Suaeda maritima* (L.) Dumort aqueous extract-mediated copper oxide nanoparticles. *Journal of Genetic Engineering and Biotechnology*, *19*(1), 131. https://doi.org/10.1186/S43141-021-00229-9/TABLES/4

[18] Tu, L. W., & Chang, K. S. (2021). Hydrothermal fabrication and photocatalytic study of delafossite ($CuFeO_2$) thin films on fluorine-doped tin oxide substrates. *Materials Chemistry and Physics*, *267*, 124620. https://doi.org/10.1016/J.MATCHEMPHYS.2021.124620

[19] Rocha, F. S., Gomes, A. J., Lunardi, C. N., Kaliaguine, S., & Patience, G. S. (2018). Experimental methods in chemical engineering: Ultraviolet-visible spectroscopy—UV-Vis. *The Canadian Journal of Chemical Engineering*, *96*(12), 2512–2517. https://doi.org/10.1002/cjce.23344

[20] Shirley, B., & Jarochowska, E. (2022). The chemical characterization is rough: The impact of topography and measurement parameters on energy-dispersive X-ray spectroscopy in biominerals. *Facies*, *68*(2), 7. https://doi.org/10.1007/s10347-022-00645-4

[21] Scimeca, M., Bischetti, S., Lamsira, H. K., Bonfiglio, R., & Bonanno, E. (2018). Energy Dispersive X-ray (EDX) microanalysis: A powerful tool in biomedical research and diagnosis. *European Journal of Histochemistry: EJH*, *62*(1), 29569878. https://doi.org/10.4081/ejh.2018.2841

[22] Ganesh Kumar, K., Balaji Bhargav, P., Ahmed, N., & Balaji, C. (2021). Influence of Sn doping on the structural, morphological, optical and photocatalytic functionality of ZnO nanostructures. *Transactions on Electrical and Electronic Materials*, *22*, 717–724.

[23] Mishra, P. K., Acharya, S., Palai, A., Sahu, S. K., Meher, A., & Sahu, D. (2024). Strategic Ni integration to study its impact on the photoluminescence and photocatalytic performances of SnO_2 nanorod architecture. *Chemistry of Inorganic Materials*, *3*, 100055. https://doi.org/10.1016/j.cinorg.2024.100055

[24] Inwati, G. K., Kumar, P., & Swart, H. C. (2022). Multifunctional properties of hybrid semiconducting nanomaterials and their applications. In V. B. Pawade, S. J. Dhoble & H. C. Swart (Eds.), *Nanoscale compound semiconductors and their optoelectronics applications* (pp. 315–350). Woodhead Publishing. https://doi.org/10.1016/B978-0-12-824062-5.00006-3

[25] Paul, M. J., Suresh, R., Sibu, G. A., Balasubramani, V., & Muthusamy, S. (2024). CuO nanoflowers: Multifaceted implications of various precipitating agents on rectification behaviour. *Optical Materials*, *152*, 115517. https://doi.org/10.1016/j.optmat.2024.115517

How to Cite: Idrees, M., Khan, S., & Hussain, S. (2025). Band Gap Modulation and Optical Property Enhancement in Sn-Doped CuO Nanostructures for Advanced Optoelectronic Applications. *Journal of Optics and Photonics Research*. https://doi.org/10.47852/bonviewJOPR52023409